Cerebral Cortex, February 2017;27: 1532–1544

doi:10.1093/cercor/bhv348
Advance Access Publication Date: 11 January 2016
Original Article

ORIGINAL ARTICLE

Asymmetry and Structure of the Fronto-Parietal Networks Underlie Visuomotor Processing in Humans

Sanja Budisavljevic[1,2], Flavio Dell'Acqua[4], Debora Zanatto[1,2], Chiara Begliomini[1,2], Diego Miotto[3], Raffaella Motta[3] and Umberto Castiello[1,2,5]

[1]Department of General Psychology, [2]Cognitive Neuroscience Center, [3]Department of Medicine, University of Padova, Padova, Italy, [4]Natbrainlab, Department of Neuroimaging, Institute of Psychiatry, Psychology and Neuroscience, King's College London, London, UK and [5]Centro Linceo Interdisciplinare, Accademia dei Lincei, Roma, Italy

Address correspondence to Sanja Budisavljevic, University of Padova, Via Venezia 8, 35131 Padova, Italy. Email: sanja.budisavljevic@gmail.com

Abstract

Research in both humans and monkeys has shown that even simple hand movements require cortical control beyond primary sensorimotor areas. An extensive functional neuroimaging literature demonstrates the key role that cortical fronto-parietal regions play for movements such as reaching and reach-to-grasp. However, no study so far has examined the specific white matter connections linking the fronto-parietal regions, namely the 3 parallel pathways of the superior longitudinal fasciculus (SLF). The aim of the current study was to explore how selective fronto-parietal connections are for different kinds of hand movement in 30 right-handed subjects by correlating diffusion imaging tractography and kinematic data. We showed that a common network, consisting of bilateral SLF II and SLF III, was involved in both reaching and reach-to-grasp movements. Larger SLF II and SLF III in the right hemisphere were associated with faster speed of visuomotor processing, while the left SLF II and SLF III played a role in the initial movement trajectory control. Furthermore, the right SLF II was involved in the closing grip phase necessary for efficient grasping of the object. We demonstrated for the first time that individual differences in asymmetry and structure of the fronto-parietal networks were associated with visuomotor processing in humans.

Key words: diffusion imaging tractography, fronto-parietal networks, reach-to-grasp, reaching, superior longitudinal fasciculus

Introduction

Simple hand movements such as reaching and reach-to-grasp are at the basis of our everyday interaction with the outside world. No matter how simple these movements seem they require specialized visuomotor mechanisms able to transform target object features into motor commands for the hand. Last couple of decades brought important insights into how the brain processes this visuomotor information (Jeannerod et al. 1995; Rizzolatti and Luppino 2001; Grafton 2010).

Research in both humans and monkeys demonstrates the fundamental role of the fronto-parietal networks for the cortical control of hand movements (Castiello 2005; Castiello and Begliomini 2008; Filimon 2010). Compared with reaching only (i.e., transport of the hand in space), reaching-to-grasp an object is characterized by both the reach and the grasp components. The latter implies hand shaping according to the target object's physical properties. Behavioral studies are consistent in showing that these 2 movements are characterized by different kinematic signatures (Marteniuk et al. 1987; Gentilucci et al. 1991). In neural terms, 2 independent fronto-parietal systems are reported to be responsible for reaching (dorsomedial network; Matelli et al. 1998; Gamberini et al. 2009; Passarelli et al. 2011) versus reach-

to-grasp movements (dorsolateral network) in both monkeys (Matelli and Luppino 2001) and humans (Filimon 2010). The dorsomedial reach pathway projects from the superior parietal lobule via the parietal reach region, which includes the superior parieto-occipital cortex (SPOC/V6A; Andersen and Buneo 2002; Buneo et al. 2002; Connolly et al. 2003), medial intraparietal sulcus, and anterior precuneus. It then extends to dorsal premotor cortex (PMd) and finally to primary motor cortex (M1). On the other hand, the dorsolateral grasp pathway projects through the anterior intraparietal sulcus to ventral premotor cortex (PMv) and from there to M1 (Jeannerod et al. 1995; Borra et al. 2008; Davare et al. 2011). However, this dual model of visuomotor processing has been put into question with recent reports of overlapping fronto-parietal activations during reaching and reach-to-grasp movements in both macaques (Fattori et al. 2009, 2010, 2012) and humans (Grol et al. 2007; Begliomini et al. 2014; Fabbri et al. 2014; Tarantino et al. 2014). Human neuroimaging studies point to bilateral hemispheric involvement of the fronto-parietal regions (Castiello and Begliomini 2008; Cavina-Pratesi et al. 2010; Glover et al. 2012; Begliomini et al. 2014) and suggest that distinct fronto-parietal networks may reflect differences in terms of motor planning and online control, rather than movement type (Grol et al. 2007; Glover et al. 2012). A point worth noting is that although the knowledge concerned with the cortical correlates behind reaching and reach-to-grasp movements in humans is extensive, a thorough exploration of the fronto-parietal connectional anatomy is lacking. The key to a more unified model of frontal and parietal networks behind reaching and reach-to-grasp movements could lie in their interconnectivity. To date, it is not known how fronto-parietal white matter networks, consisting of the 3 parallel pathways of the superior longitudinal fasciculus (SLF), support visuomotor processing in humans.

The SLF is a major bidirectional association tract that covers an extensive range of areas in the frontal and the parietal lobes. It was first described in the monkey brain using autoradiographic technique (Petrides and Pandya 1984), and later in the human brain using diffusion imaging tractography (Makris et al. 2005; Thiebaut de Schotten et al. 2011, 2012; Jang and Hong 2012; Kamali et al. 2014; Wang et al. 2015) and postmortem dissections (Thiebaut de Schotten et al. 2011; Wang et al. 2015). The SLF is subdivided into 3 branches on the basis of its course and cortical terminations. According to previous studies in humans (Thiebaut de Schotten et al. 2011; Rojkova et al. 2015), the superior branch (SLF I) originates from the precuneus and the superior parietal lobule (Brodmann areas, BA5 and BA7) and projects to the superior frontal gyrus (BA6, BA8, BA9 up to BA10). The middle pathway (SLF II) connects the inferior parietal lobe (angular gyrus and intraparietal sulcus—BA39) and the posterior regions of the middle frontal gyrus (BA6), with some projections continuing anteriorly to BA46. Lastly, the inferior branch (SLF III) originates in the inferior parietal lobe (supramarginal gyrus, BA40) and terminates in the pars opercularis (BA44), triangularis (BA45) and the inferior frontal gyrus (BA47). The exact roles and significance of the 3 SLF subcomponents in the visuomotor processing are not known, although it has been suggested that fronto-parietal connections might be crucial for the planning of reach-to-grasp actions (Koch et al. 2010).

The focus of the current study is to bridge the gap between the relatively detailed knowledge of the cortical mechanisms and the limited understanding of the corresponding fronto-parietal white matter networks behind reaching and reach-to-grasp actions. We recruited 30 healthy right-handed participants and used diffusion magnetic resonance imaging tractography, based on the spherical deconvolution approach (Dell'Acqua et al. 2010), to delineate the 3 branches of the SLF. For the same participants, we separately recorded kinematics of reaching and reach-to-grasp movements of their dominant right hand. We explored the correlations between asymmetry and anatomy (i.e., volumetric measures) of the SLF branches and the movement kinematics, and investigated possible differential effects of the SLF anatomy on reaching versus reach-to-grasp kinematic markers. According to the original dual model of visuomotor processing, we would expect to find a significant relationship between reaching and the connections to the PMd (SLF II), whereas connections to the PMv (SLF III) would be specifically tailored to support the grasp component of the action. However, in light of the recent functional neuroimaging literature in humans, we expected to observe significant correlations between bilateral SLF II and SLF III and the kinematic markers of both reaching and reach-to-grasp movements. Having in mind the important role of the right PMd for grasping (Begliomini et al. 2008, 2014) and the right intraparietal sulcus for processing finger configurations and the final contact points with the object during grasping (Hermsdörfer et al. 2001; for a review, see Castiello 2005), we hypothesized that the connections between these regions, that is, the right SLF II, could be associated with the grasp components of the reach-to-grasp action. Lastly, reaching and reach-to-grasp movements present a useful tool to study hemispheric specialization, since they incorporate both motor coordination and visuomotor transformations and show bilateral involvement of the fronto-parietal regions. Thus, we investigated how the lateralization of the 3 SLF branches is associated with the kinematics of the considered hand actions.

Materials and Methods

Participants

A sex- and age-balanced sample of 30 healthy participants (14 males, 16 females; mean age 24.6 ± 2.8, age range: 20–31 years) was recruited. All participants were right-handed according to the Edinburgh Handedness Inventory (Oldfield 1971), which ranges from −100 for purely left handed to +100 for purely right-handed participant. Demographic data together with the handedness scores are reported in Supplementary Table 1. No history of neurological and psychiatric disorders was present in the study sample. All participants gave informed written consent in accordance with the ethics approval by the Institutional Review Board at the University of Padova, in accordance with the Declaration of Helsinki (Sixth revision, 2008).

Behavioral Experiment

Task and Stimulus

Participants were requested to perform 2 tasks: a reach-to-grasp task, in which they were asked to reach toward and grasp the object with a precision grip, and a reaching task in which they were asked to perform a movement toward the stimulus and touch the object's frontal surface with their knuckles, maintaining the hand in a closed fist (Fig. 1). The fist's posture was chosen as to minimize distal involvement. Participants fixated the target object during both the reaching and the reach-to-grasp actions. The stimulus consisted of a spherical object (2 cm diameter) that would normally be grasped with a precision grip (PG; using the index finger and thumb). All participants were explicitly asked to use a PG for grasping the object. Participants were informed as to which task to perform by an auditory cue (high-pitch: reach-to-grasp; low-pitch: reaching). The sound also had

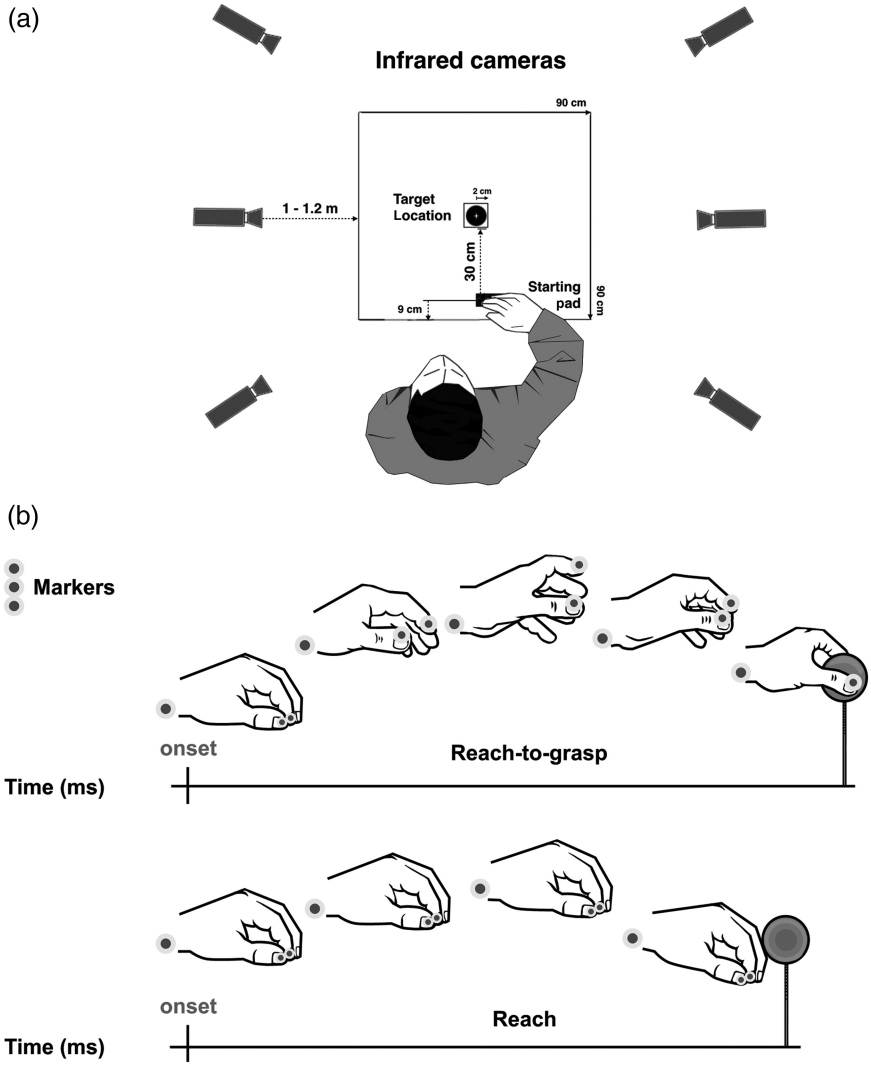

Figure 1. Descriptive example of the experimental set-up showing (*a*) designated start position for (*b*) reach-to-grasp and reaching movements.

a "go-signal" function in the sense that participants were asked to start their actions toward the object only after the sound was delivered. Trials in which the participants did not comply with the task or did not fixate the target were not included in the analysis.

Procedure

Each participant sat on a height-adjustable chair in front of a table (900 × 900 mm) with the elbow and wrist resting on the table surface and the right hand in the designated start position (Fig. 1). The hand was pronated with the palm resting on a pad (60 × 70 mm), which was shaped to allow for a comfortable and repeatable posture of all digits, that is, slightly flexed at the metacarpal and proximal interphalangeal joints. The starting pad was attached 90 mm away from the edge of the table surface. The object was placed on a platform located at a distance of 300 mm between the platform and the sagittal plane of the hand's starting position on the right side of the table.

Kinematics Recording

A 3D-Optoelectronic SMART-D system (Bioengineering Technology and Systems, BTS) was used to track the kinematics of the participant's right upper limb. Three light-weight infrared reflective markers (0.25 mm in diameter; BTS) were taped to the following points: 1) thumb (ulnar side of the nail); 2) index finger (radial side of the nail); and 3) wrist (dorsodistal aspect of the radial styloid process). Six video cameras (sampling rate 140 Hz) detecting the markers were placed in a semicircle at a distance of 1–1.2 m from the table. The camera position, roll angle, zoom, focus, threshold, and brightness were calibrated and adjusted to optimize marker tracking, followed by static and dynamic calibration. For the static calibration, a 3-axes frame of 5 markers at known distances from each other was placed in the middle of the table. For the dynamic calibration, a 3-marker wand was moved throughout the workspace of interest for 60 s. The spatial resolution of the recording system was 0.3 mm over the field of view. The standard deviation of the reconstruction error was below 0.2 mm for the *x*-, *y*-, and *z*-axes.

Data Processing

Following data collection, each trial was individually checked for correct marker identification, and the SMART-D Tracker software package (BTS) was used to provide a 3-D reconstruction of the marker positions as a function of time. The data were then

filtered using a finite impulse response linear filter (transition band = 1 Hz, sharpening variable = 2, cutoff frequency = 10 Hz; D'Amico and Ferrigno, 1990; 1992). Movement onset was defined as the time at which the tangential velocity of the wrist marker crossed a threshold (5 mm/s) and remained above it for longer than 500 ms. For the reach-to-grasp task, the end of movement was defined as the time at which the hand made contact with the object and quantified as the time at which the hand opening velocity crossed a threshold (−5 mm/s) after reaching its minimum value and remained above it for longer than 500 ms. For the reaching task, the end of movement was defined as the time at which the hand made contact with the object and quantified as the time at which the wrist velocity crossed a threshold (5 mm/s) after reaching its minimum value and remained above it for longer than 500 ms. For both reaching and reach-to-grasp tasks, the following kinematic parameters were extracted for each individual movement using a custom protocol run in Matlab 2014b (The 4 MathWorks, Natick, MA, USA): the time interval between movement onset and end of movement (Movement Time), the time at which the tangential velocity of the wrist was maximum from movement onset (Time to Peak Wrist Velocity) and its amplitude (Amplitude of Maximum Peak Velocity), the time at which the acceleration of the wrist was maximum from movement onset (Time to Peak Acceleration) and its amplitude (Amplitude of Maximum Peak Acceleration), and the time at which the deceleration of the wrist was maximum from movement onset (Time to Peak Deceleration) and its amplitude (Amplitude of Maximum Peak Deceleration). For the reach-to-grasp task, 3 grasp-specific measures were assessed, namely the time at which the distance between the 3D coordinates of the thumb and index finger was maximum, between movement onset and hand contact time (Time to Maximum Grip Aperture); and the time and amplitude of the maximum closing grip velocity.

MRI Data Acquisition

Diffusion imaging data were acquired using a Siemens Avanto 1.5 T scanner housed in Padova University Hospital with actively shielded magnetic field gradients (maximum amplitude 45 mT/m). The body coil was used for RF transmission and an 8-channel head coil for signal reception. Protocol consisted of a localizer scan, followed by a single-shot, spin-echo, EPI sequence with the following parameters: TR = 8500, TE = 97, FOV = 307.2 × 307.2, matrix size = 128 × 128, 60 slices (no gaps) with isotropic (2.4 × 2.4 × 2.4 mm^3) voxels. The maximum diffusion weighting was 2000 s/mm^2, and at each slice location, 7 images were acquired with no diffusion gradients applied ($b = 0$ s/mm^2), together with 64 diffusion-weighted images in which gradient directions were uniformly distributed in space and repeated 3 times, to increase signal to noise ratio (SNR). Gains and scaling factors were kept constant between acquisitions. Scanning lasted approximately 30 min.

Correction of Motion and Eddy Current Distortion, and Estimation of the Fiber Orientation Distribution

Each subject's raw image data were examined before proceeding on to further analyses to detect any outliers in the data, including signal drop-outs, poor signal-to-noise ratio, and image artifacts such as ghosts. Any subject whose raw data contained volumes with significant image quality issues was removed from further analyses. The remaining 30 participants were processed as follows.

The 4 repeated DWI datasets were concatenated and corrected for subject motion and geometrical distortions using ExploreDTI (http://www.exploredti.com; Leemans et al. 2009). Spherical deconvolution (Tournier et al. 2004, 2007) approach was chosen to estimate multiple orientations in voxels containing different populations of crossing fibers (Alexander 2005). Spherical deconvolution was calculated applying the damped version of the Richardson–Lucy algorithm with a fiber response parameter $\alpha = 1.5$, 200 algorithm iterations, and $\eta = 0.15$ and $\nu = 15$ as threshold and geometrical regularization parameters (Dell'Acqua et al. 2010). An example of the recovered fiber orientation distribution (FOD) profiles obtained with these settings is provided in the Supplementary Fig. 1. Fiber orientation estimates were obtained by selecting the orientation corresponding to the peaks (local maxima) of the FOD profiles. To exclude spurious local maxima, we applied both an absolute and a relative threshold on the FOD amplitude (Dell'Acqua et al. 2013). The first "absolute" threshold corresponding to a Hindrance Modulated Orientational Anisotropy (HMOA) threshold of 0.015 was used to exclude intrinsically small local maxima due to noise or partial volume effects with isotropic tissue. This threshold was set to select only the major fiber orientation components and exclude low amplitude spurious FOD components obtained from gray matter and cerebro-spinal fluid isotropic voxels. The second "relative" threshold of 5% of the maximum amplitude of the FOD was applied to remove remaining unreliable local maxima with values greater than the absolute threshold but still significantly smaller than the main fiber orientation (Dell'Acqua et al. 2013).

Tractography Algorithm

Whole brain tractography was performed selecting every brain voxel with at least 1 fiber orientation as a seed voxel. From these voxels, and for each fiber orientation, streamlines were propagated using a modified Euler integration with a step size of 1 mm. When entering a region with crossing white matter bundles, the algorithm followed the orientation vector of the least curvature. Streamlines were halted when a voxel without fiber orientation was reached or when the curvature between 2 steps exceeded a threshold of 45°. All spherical deconvolution and tractography processing was performed using StarTrack (http://www.natbrainlab.com), a freely available Matlab software toolbox developed by Flavio Dell'Acqua at NatBrainLab, King's College London, and based on the methods described in Dell'Acqua et al. (2013).

Tractography Dissections of Parieto-Frontal Network

To visualize fiber tracts and quantify tract-specific measures, we used TrackVis software (http://www.trackvis.org; Wang et al. 2007). We used a multiple regions of interest (ROIs) approach to isolate different subcomponents of the fronto-parietal SLF network according to a dissection method previously described in Thiebaut de Schotten et al. (2011). Three separate coronal ROIs were manually delineated on the FA map of each subject: around the white matter of the superior frontal gyrus (Sfg ROI), the middle frontal gyrus (MFg ROI), and the inferior/precentral frontal gyrus (Prg ROI); another "AND" ROI was delineated posteriorly encompassing the parietal area (Pa ROI) (see Supplementary Fig. 2). The "AND" ROI is used to represent an obligatory passage for a tract and to include the desired streamlines (passing though the first ROI and the "AND" ROI), while a "NOT" ROI is used to exclude undesired streamlines (not displaying fibers passing though the first ROI and the "NOT" ROI). For all the tracts, that

is SLF I, SLF II, and SLF III, streamlines of the arcuate fasciculus projecting to the temporal lobe were excluded using a "NOT" ROI in the temporal white matter (the arcuate is not part of the parieto-frontal system as it projects to the temporal lobe). The most dorsal component SLF I was dissected as a tract connecting the superior frontal gyrus to the parietal regions (Sfg ROI and Pa ROI) while excluding the streamlines from the cingulum bundle using another "NOT" ROI (cingulum fibers lie inferior to the SLF I fibers). The middle SLF II was dissected by connecting the middle frontal gyrus to the parietal area (MFg ROI and Pa ROI), and lastly the most ventral branch—SLF III as a tract connecting the inferior/precentral frontal regions to the parietal cortex (Prg ROI and Pa ROI).

Statistical Analysis

Statistical analysis was performed using SPSS software (Version 21) (SPSS, Chicago, IL, USA). Gaussian distribution was confirmed for all kinematic and tractography dependent variables using the Shapiro–Wilk test (α-level: $P < 0.05$, minimum $P = 0.062$) (Shapiro and Wilk 1965) allowing the use of parametric statistics. The mean value for each kinematic parameter of interest was determined based on 12 individual observations for each participant and then entered into separate paired-samples *t*-tests for comparing reaching versus reach-to-grasp conditions. To estimate the effect size, we calculated Cohen's *d* for dependent *t*-tests, from formula described in Dunlop et al. (1996, S. 171)—as cited and calculated at: http://www.psychometrica.de/effect_size.html#dep.

The number of streamlines (NoS) within the tract of interest and volume (Vol; the number of voxels, proxy for volume) through which the fibers pass were extracted for each SLF tract. There are several shortcomings when using only one of these measures in tractography studies. It is known that the NoS can be affected by different features of the pathway (curvature, length, width, myelination) and experimental conditions (e.g., local variations in SNR) (Jones et al. 2012). The streamlines count approach favors the shortest, straightest, and simplest paths, thus potentially biasing the NoS measures. On the other hand, the Vol measures considers the spatial extent of the pathway by counting the number of voxels intersected by streamlines. This means that more spread out the streamlines are, the larger the number of voxels and the Vol (Jones and Cercignani 2010). However, the uncertainty in fiber orientation can affect the spread of the streamlines, and thus bias the volume measures, making it a misleading parameter. To the best of our knowledge, there is no method to correct for the kinds of problems related to the NoS and the Vol measures. Until such methods are developed, we have opted to use both of these measures in our analysis to increase the confidence in our findings. As expected, Vol and NoS measures were significantly correlated in our data (r range = 0.841–0.920). To account for individual variations in brain size and gender differences, NoS and Vol measures were normalized by the total NoS and total white matter Vol obtained from the full brain tractography. Lateralization index (LI) for the 3 SLF branches was calculated according to the previously published formula (Thiebaut de Schotten et al. 2011) for both Vol and NoS measures: LI_{Vol} = (Right Vol – Left Vol)/(Right Vol + Left Vol) for the lateralization of the Vol, and LI_{NoS} = (Right NoS – Left NoS)/(Right NoS + Left NoS) for the lateralization of the NoS. Negative values indicate greater NoS or Vol in the left hemisphere, while positive values indicate right lateralization of NoS or Vol. Values around zero indicate a similar NoS or Vol between the left and the right hemisphere. Statistical significance of the degree of the lateralization index was determined using a 1-sample *t*-test (test value = 0) for each SLF tract. Pearson's bivariate correlation analysis was used to detect the strength of the correlation between the tract-specific measures and the kinematic markers of reaching and reach-to-grasp movements. However, all significant findings were replicated also using a robust Spearman's correlation technique before being reported in the results. Due to dependency of volumetric measures (NoS and Vol), we employed a false discovery rate (FDR) correction (Benjamini and Hochberg 1995) for 6 comparisons using the q-value of 0.05 for significant results (FDR $P < 0.05$). We used Fisher's r-to-z transformation and asymptotic *z*-test to statistically test the difference between the 2 dependent correlations with 1 variable in common (Lee and Preacher 2013). Degree of manual dominance (ranging from +70 to +100; see Supplementary Table 1) had no significant effect on the measured variables and the correlations reported.

Results

Behavioral Results

Means, standard deviations, and statistical tests are summarized in Table 1. We explored the determinants of the movement kinematics by comparing the conditions, in which the participants

Table 1 Movement time and kinematic values showing statistically significant differences between the reach and the reach-to-grasp conditions

Variable	M ± SD		*t* (df)	P
	Reach	Reach-to-grasp		
Movement time (ms)	654 ± 55	730 ± 56	−17.6 (29)	<0.0001
Time to peak velocity (ms)	264 ± 23	309 ± 24	−13.9 (29)	<0.0001
Time to peak acceleration (ms)	165 ± 15	219 ± 12	−19.1 (29)	<0.0001
Time to peak deceleration (ms)	424 ± 30	504 ± 21	−15.1 (29)	<0.0001
Amplitude peak velocity (mm/s)	812 ± 52	693 ± 61	12.6 (29)	<0.0001
Amplitude peak acceleration (mm/s^2)	7901 ± 252	6702 ± 476	20.8 (29)	<0.0001
Amplitude peak deceleration (mm/s^2)	7490 ± 387	6457 ± 459	18.1 (29)	<0.0001
Time to maximum grip aperture (ms)	n/a	509 ± 22	n/a	n/a
Time of closing grip velocity (ms)	n/a	684 ± 29	n/a	n/a
Amplitude of closing grip velocity (mm/s^2)	n/a	−396 ± 68	n/a	n/a

Note: Time to maximum grip aperture and time and amplitude of closing grip velocity were measured only for the reach-to-grasp condition. *M* = means, SD = standard deviation, *P* = *P* value after Bonferroni correction.

were requested to reach toward and grasp the object (reach-to-grasp) or solely reach the object (Fig. 1). For all 7 considered dependent measures, a statistically significant effect of the task was found. Movement time was shorter for the reaching than for the reach-to-grasp task ($t_{(29)} = -17.6$, $P < 0.0001$, $d = 1.38$). Also, the time to peak velocity ($t_{(29)} = -13.9$, $P < 0.0001$, $d = 1.86$), acceleration ($t_{(29)} = -19.1$, $P < 0.0001$, $d = 3.79$), and deceleration ($t_{(29)} = -15.1$, $P < 0.0001$, $d = 3.01$) were reached earlier for reaching than for reach-to-grasp condition. The amplitude of peak velocity ($t_{(29)} = 12.6$, $P < 0.0001$, $d = 2.06$), acceleration ($t_{(29)} = 20.8$, $P < 0.0001$, $d = 2.45$), and deceleration ($t_{(29)} = 18.1$, $P < 0.0001$, $d = 2.38$) were higher for the reaching than for the reach-to-grasp task.

Diffusion Imaging Tractography Results

Anatomical Lateralization of the SLF Pathways

An example of the SLF dissection in the right hemisphere of a representative subject is shown in Figure 2*a*. By measuring the volumes (Vol) and the NoS of the tracts in both hemispheres, we calculated the lateralization index (LI_{NoS} and LI_{Vol}) of the 3 SLF branches. Different lateralization patterns for the 3 SLF segments were observed (Fig. 2*b*). SLF I showed statistically significant left lateralization ($LI_{NoS} = -0.132 \pm 0.251$, $t_{(29)} = -2.888$, $P = 0.007$; $LI_{Vol} = -0.075 \pm 0.187$, $t_{(29)} = -2.201$, $P = 0.036$); SLF II was symmetrically distributed between the left and the right hemisphere ($LI_{NoS} = 0.014 \pm 0.272$, $t_{(29)} = 0.322$, $P = 0.750$; $LI_{Vol} = -0.002 \pm 0.151$, $t_{(29)} = -0.050$, $P = 0.961$), while the SLF III was significantly right lateralized ($LI_{NoS} = 0.357 \pm 0.203$, $t_{(29)} = 9.652$, $P < 0.0001$; $LI_{Vol} = 0.200 \pm 0.152$, $t_{(29)} = 7.216$, $P < 0.0001$). We performed additional analyses on the asymmetry of diffusion measures that reflect the microstructural properties of the SLF tracts. At the group level, fractional anisotropy (FA) was left lateralized in SLF I ($LI_{FA} = -0.035 \pm 0.037$, $t_{(29)} = -5.156$, $P < 0.0001$), but significantly higher in the right hemisphere for SLF II ($LI_{FA} = 0.027 \pm 0.038$, $t_{(29)} = 3.902$, $P = 0.001$) and SLF III ($LI_{FA} = 0.021 \pm 0.035$, $t_{(29)} = 3.237$, $P = 0.003$). Mean diffusivity (MD) exhibited a reverse distribution and was significantly higher in the right SLF I ($LI_{MD} = 0.005 \pm 0.007$, $t_{(29)} = 4.454$, $P < 0.0001$), and the left SLF II ($LI_{MD} = -0.006 \pm 0.009$, $t_{(29)} = -3.829$, $P = 0.001$) and SLF III ($LI_{MD} = -0.007 \pm 0.006$, $t_{(29)} = -6.375$, $P < 0.0001$).

Relating Inter-Individual Differences in Movement Kinematics to Asymmetry and Anatomy of the Fronto-Parietal Pathways

We found significant correlations between the lateralization of the SLF II, volumetric measures of the bilateral SLF II and SLF III, and the kinematics of the reaching and reach-to-grasp movements. Correlations between the SLF I and the kinematic parameters were not statistically significant (see Supplementary Fig. 4).

Relationship with SLF II Hemispheric Distribution

We observed significant correlations between the SLF II lateralization and the acceleration amplitude of movement (Table 2). It should be noted that although at the group level the SLF II was symmetrically distributed (Fig. 2*c*), the inter-individual variability was very high, ranging from −0.40 to 0.53 for LI_{NoS}, and

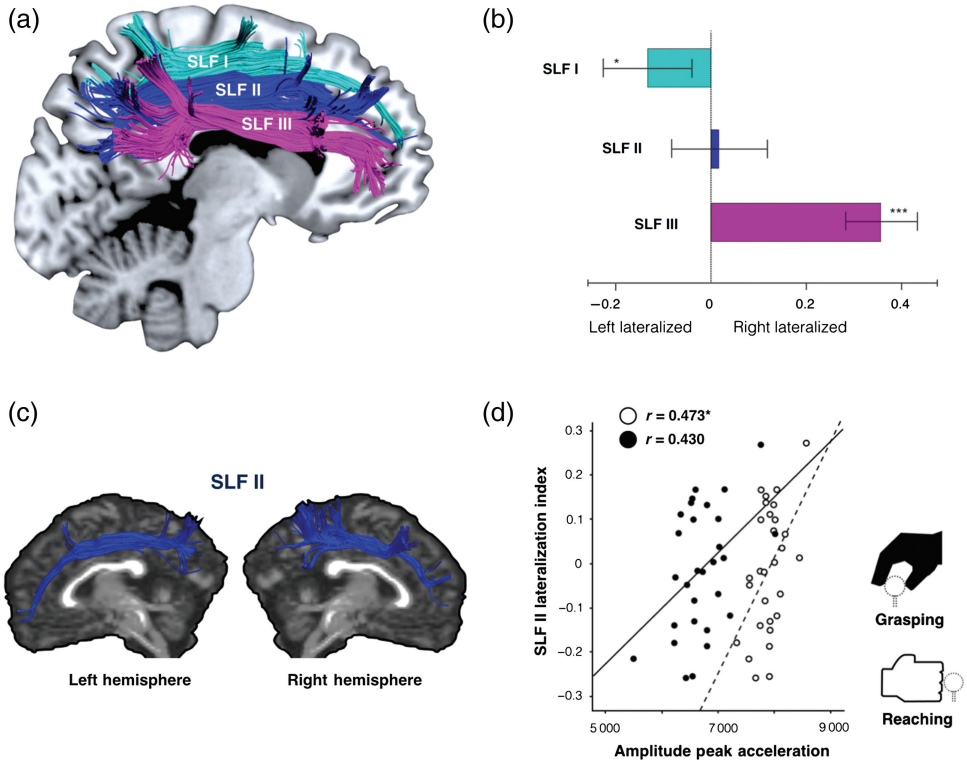

Figure 2. (*a*) Tractography reconstruction of the fronto-parietal connections in the right hemisphere of a representative subject showing the most dorsal branch SLF I (light blue), the middle component SLF II (navy blue), and the ventral component SLF III (violet) (*b*) Hemispheric lateralization of the 3 branches with the corresponding 95% confidence intervals showing left lateralization of the SLF I, symmetrical distribution of the SLF II, and right lateralization of the SLF III (lateralization index based on the NoS, *$P < 0.01$, ***$P < 0.001$) (*c*) Symmetrical hemispheric distribution of the SLF II in 1 representative subject. (*d*) Correlations between the lateralization of the SLF II volume and the amplitude of peak acceleration during reaching and reach-to-grasp movements. *$P < 0.01$ (FDR $P < 0.05$ corrected).

Table 2 Correlations between volumetric measures of the bilateral SLF II and SLF III and kinematic variables, with Pearson's correlation coefficient *r* and *P* value in brackets

Tract		Movement time		Time to peak deceleration	Amplitude of peak velocity		Amplitude of peak acceleration		Amplitude of closing grip velocity	Maximum grip aperture
		R	RG	RG	R	RG	R	RG	RG	RG
Left SLF II	NoS	—	—	—	—	—	**−0.511*** **(0.005)**	−0.388 (0.042)	—	—
	Vol	—	—	—	—	—	−0.410 (0.030)	−0.298 (0.124)	—	—
SLF III	NoS	—	—	—	—	—	0.274 (0.158)	0.442 (0.018)	—	—
	Vol	—	—	—	—	—	0.441 (0.019)	**0.518*** **(0.005)**	—	—
Right SLF II	NoS	−0.403 (0.030)	**−0.457*** **(0.013)**	**−0.518*** **(0.005)**	—	—	—	—	−0.261 (0.171)	−0.400 (0.035)
	Vol	−0.354 (0.064)	**−0.454*** **(0.015)**	**−0.480*** **(0.010)**	—	—	—	—	**−0.500*** **(0.007)**	−0.233 (0.215)
SLF III	NoS	−0.443 (0.018)	**−0.522*** **(0.004)**	—	**0.493*** **(0.007)**	0.406 (0.029)	—	—	—	—
	Vol	−0.389 (0.041)	**−0.510*** **(0.006)**	—	**0.571*** **(0.002)**	0.447 (0.015)	—	—	—	—
Lat. Index SLF II	NoS	—	—	—	—	—	**474*** **(0.009)**	0.395 (0.034)	−0.231 (0.246)	−0.406 (0.032)
	Vol	—	—	—	—	—	**0.473*** **(0.010)**	0.430 (0.020)	−0.389 (0.045)	−0.218 (0.266)

Note: R, reach; RG, reach-to-grasp; LI, lateralization index; NoS, number of streamlines; Vol, volume.
*Correlations that survived FDR $P < 0.05$ correction.

−0.25 to 0.31 for LI_{Vol} (the minimum and maximum values represent significant left and right lateralization, respectively). Individuals with larger SLF II in the right hemisphere relative to the left, tended to have significantly higher acceleration amplitude of reaching movements. For the reach-to-grasp condition, the correlations with the acceleration amplitude were also significant, but they did not survive the correction for multiple comparisons (Table 2). The correlations were not significantly different between the 2 movement conditions ($z_{NoS} = 0.69$, $P = 0.693$; $z_{Vol} = 0.394$, $P = 0.693$) (for a scatterplot of the correlations, see Fig. 2*d*). Lastly, significant correlations were found between the SLF II lateralization and the grasp-specific measures, that is, time to maximum grip aperture and the amplitude of closing grip velocity, but they did not survive the FDR correction (Table 2).

Relationship with SLF II and SLF III in the Left Hemisphere

We observed significant associations between volumetric measures of the SLF II and the SLF III in the left hemisphere and the acceleration amplitude of reaching and reach-to-grasp movements (Table 2).

Higher NoS in the left SLF II corresponded to lower acceleration amplitudes of reaching movements (Fig. 3), in line with our results on the SLF II lateralization. Significant correlation was also found for the acceleration amplitude of the reach-to-grasp movement, but it did not survive the FDR correction. Nevertheless, there was no significant difference between reaching and reach-to-grasp correlations with the left SLF II ($z_{NoS} = -1.09$, $P = 0.275$). Before the FDR correction, correlation with the Vol measures of the left SLF II was also significant (reaching condition).

Regarding the ventral SLF branch, larger volumes of the left SLF III corresponded to higher acceleration amplitudes of the reach-to-grasp movements. For the reaching condition, correlation was also significant, but it did not survive the FDR correction (Table 2). The difference between the 2 correlations was not significant ($z_{Vol} = 1.003$, $P = 0.315$) (for a scatterplot of the correlations, see Fig. 3). Before the FDR correction, correlation with the NoS of the left SLF III was also significant for the reach-to-grasp condition (Table 2).

Relationship with SLF II and SLF III in the Right Hemisphere

A significant relationship was found between the anatomy of the SLF II and the SLF III in the right hemisphere and the kinematic measures that reflect the temporal aspects of movement (SLF II, SLF III) or the grasp-specific measures (SLF II) (Table 2).

The structure of the SLF II and the SLF III in the right hemisphere was significantly related to the total movement time in the reach-to-grasp condition. In the reaching condition, the correlations were also significant but failed to survive the multiple comparisons correction (Table 2). Thus, larger SLF II and SLF III in the right hemisphere, in terms of Vol and NoS, corresponded to faster reach-to-grasp movements. However, there were no significant differences between the correlations for the reach versus reach-to-grasp movement times for both the SLF II ($z_{NoS} = 0.73$, $P = 0.465$; $z_{Vol} = 1.29$, $P = 0.197$) and the SLF III ($z_{NoS} = 1.066$, $P = 0.286$; $z_{Vol} = 1.609$, $P = 0.107$) (for a scatterplot of the correlations, see Fig. 3). Furthermore, the larger right SLF II, in terms of Vol and NoS, corresponded to shorter time to peak deceleration for reach-to-grasp movements. No significant differential effect was observed in relation to the reaching condition where correlation was not significant ($z_{NoS} = -0.707$, $P = 0.479$;

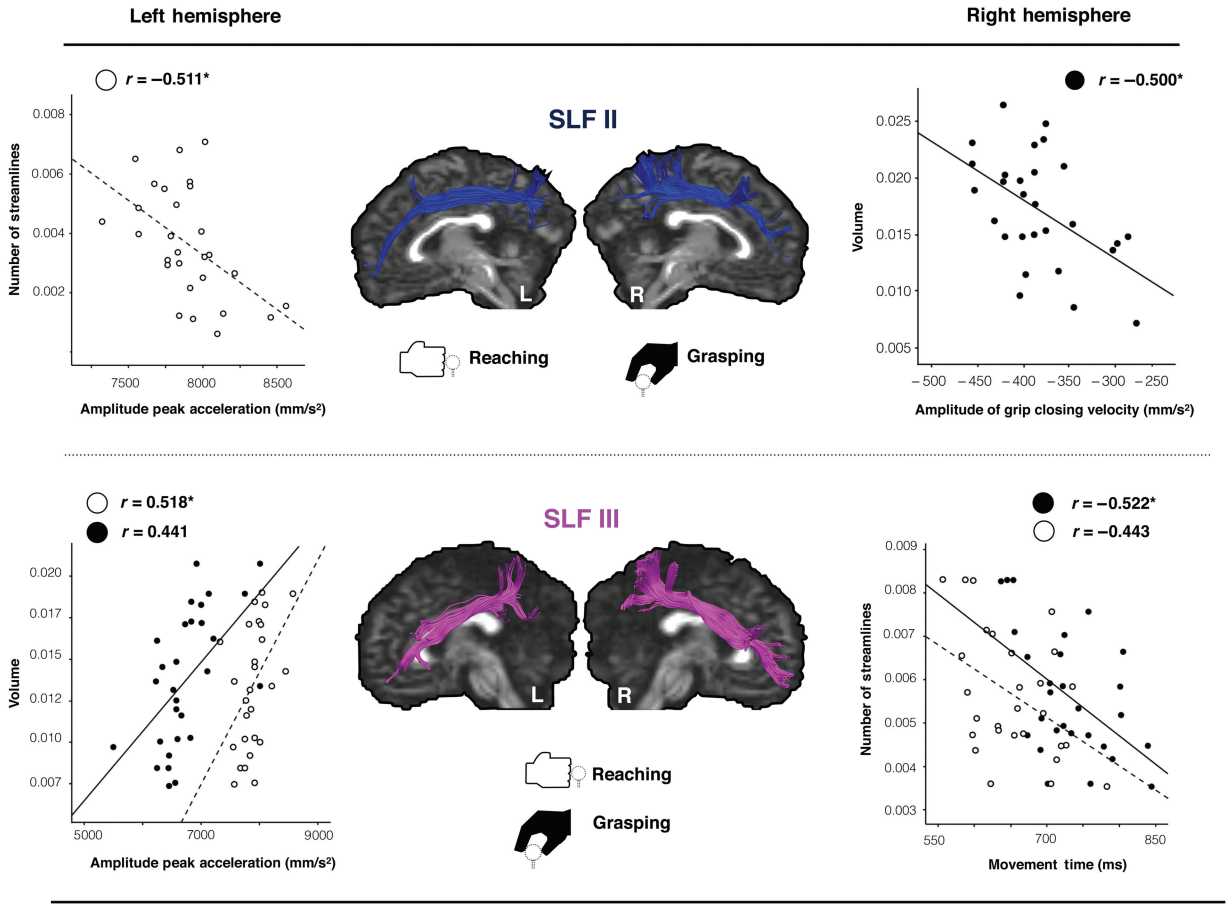

Figure 3. Correlations between the kinematic variables of reaching and reaching-to-grasp (i.e., movement time (ms), amplitudes of peak acceleration and closing grip velocity (mm/s^2)), and the volumetric measures of the bilateral SLF II and SLF III. *$P < 0.01$ (FDR $P < 0.05$ corrected).

$z_{Vol} = -1.351$, $P = 0.176$). On the other hand, the larger right SLF III, in terms of Vol and NoS, corresponded to higher velocity amplitudes for reaching movements. The correlation was also significant for the reach-to-grasp condition, but it did not survive the FDR correction. There was no significant difference between the correlations of the 2 conditions ($z_{NoS} = 0.561$, $P = 0.574$; $z_{Vol} = 0.842$, $P = 0.399$).

Lastly, the right SLF II was significantly associated with the grasp component of the reach-to-grasp action. Larger volumes (but not the NoS) of the right SLF II corresponded to lower amplitudes of closing grip velocity during grasping phase of movement (Fig. 3). In contrast, the correlation with the left SLF II was not significant ($r_{Vol} = -0.112$, $P = 0.564$), and this difference between left and right SLF II was significant ($z_{Vol} = -2.231$, $P = 0.02$). Correlation of the right SLF II and another grasp-specific measure, that is, the time to maximum grip aperture, was also significant, but it did not survive the FDR correction (Table 2).

Discussion

Our results showed that asymmetry and structure of the fronto-parietal white matter networks affect the visuomotor processing in humans. The findings suggested that the second and the third branch of the superior longitudinal fasciculus (SLF II and SLF III) support both reaching and reach-to-grasp movements. Larger SLF II and SLF III in the right hemisphere were related to faster visuomotor processing, while the left SLF II and SLF III played a role in initial trajectory features such as movement acceleration. Furthermore, the right SLF II was involved in the closing grip phase of the reach-to-grasp movement, necessary for efficient and stable contact with the target object.

Our behavioral results are consistent with the published literature in showing that reach and reach-to-grasp movements significantly differ in terms of kinematics (Marteniuk et al. 1987; Gentilucci et al. 1991; Castiello 2001). In neural terms, a lack of functional fronto-parietal segregation was observed in monkeys (Galleti et al. 2003; Fattori et al. 2004, 2009, 2010, 2012) and humans (Grol et al. 2007; Begliomini et al. 2014; Fabbri et al. 2014; Tarantino et al 2014). Our findings further argue against the dual model of visuomotor processing of the reach and the grasp components. We showed that the ventral SLF III correlated not only with the reach-to-grasp kinematics, but also with the reaching movement; while the SLF II was not only associated with the reaching kinematics, but also with the grasp-specific components of the action.

The key position of the SLF II and SLF III, linking inferior parietal regions and frontal premotor areas, points to both pathways playing a role in reach and reach-to-grasp actions. The SLF II originates in the angular gyrus and intraparietal sulcus, previously associated with the preparation of reaching movements (Jeannerod et al. 1995; Castiello 2005; Karnath and Perenin 2005) but also with the integration of grasp-relevant information (Tarantino et al. 2014; Monaco et al. 2014). The SLF II then courses through the supramarginal gyrus where the SLF III emerges, a

region implicated in a variety of reach-to-grasp-related functions such as precision grasping (Binkofski et al. 1998; Culham and Valyear 2006; Olivier et al. 2007; Begliomini et al. 2007), online monitoring and control (Glover et al. 2012), and motor attention (Rushworth et al. 1997, 2001; Martin et al. 2011). From there, the SLF II runs to the middle frontal gyrus and dorsal premotor areas important for planning (Glover et al. 2012) and execution (Buxbaum et al. 2006; Begliomini et al. 2014) of reach-to-grasp movements as well as other motor-related functions, for example action selection (Lau et al. 2004), active representation of motor plans (Curtis and D'Esposito 2003), and hand movement sequencing (Davare et al. 2006). On the other hand, the SLF III runs to the ventral premotor regions supporting visuomotor transformations for correct hand posture during grasping (Davare et al. 2006; Raos et al. 2006) and reaching direction (Kakei et al. 2001). The SLF tracts are bidirectional, confirming their role not only in linking sensory representations to relevant motor maps but also in a top–down control of movements.

The observed bilateral SLF II and SLF III involvement in our study parallels the findings from functional neuroimaging and transcranial magnetic stimulation studies on bilateral involvement of the fronto-parietal regions that SLF II and SLF III connect during reach and reach-to-grasp movements (Ehrsson et al. 2000, 2001; Davare et al. 2006, 2007; Castiello and Begliomini 2008; Cavina-Pratesi et al. 2010; Glover et al. 2012; Begliomini et al. 2014). Our results give support to the bi-hemispheric model of motor lateralization (Sainburg 2002), where the non-dominant right hemisphere is related to the temporal aspects of movement (Haaland et al. 1999) and grasp-preshaping (Tretriluxana et al. 2008), while the left hemisphere is associated with the movement trajectory features (Sainburg and Kalakanis 2000; Sainburg 2002; Sainburg and Wang 2002; Haaland et al. 2004).

Relating Variation in Kinematics to SLF II and SLF III in the Left Hemisphere

The left SLF II and SLF III were significantly associated with the movement acceleration amplitude, with no differential effect on reaching versus reach-to-grasp condition. Our findings are in line with previous reports showing that left-hemisphere damage impairs the movement acceleration (Fisk and Goodale 1988; Mattingley et al. 1994; Haaland and Harrington 1989; Winstein and Pohl 1995) and modulates the acceleration amplitude (Schaefer et al. 2007) and coordination of proximal muscles that support the movement acceleration (Robertson et al. 2012). Our study lends support to the notion that the left hemisphere and its connections are important for the control of movement trajectories (Haaland et al. 2004) and limb dynamics (Tretriluxana et al. 2008; Sainburg and Kalakanis 2000, Bagesteiro and Sainburg 2002, 2003; Sainburg 2002; Sainburg and Wang 2002) underlying movement acceleration. Overall, the left SLF II and SLF III connections might be involved in specifying the initial trajectory features of reach and reach-to-grasp movements that relate to the dynamic properties of the arm.

Relating Variation in Kinematics to SLF II and SLF III in the Right Hemisphere

We found significant associations between the SLF II and the SLF III in the right hemisphere and kinematic markers that reflect the temporal aspects of movement (SLF II, SLF III) or the grasp-specific measures (SLF II). Larger SLF II and SLF III in the right hemisphere corresponded to faster speed of reach and reach-to-grasp movements. Moreover, larger SLF III in the right hemisphere corresponded to both faster movement and higher velocity amplitudes. Control of movement velocity during action execution is an important aspect of temporal coordination, and patients with right hemispheric damage often have impairments of velocity control and require longer time to terminate their movements (Mattingley et al. 1994; Konczak and Karnath 1998). Overall, the present results support the notion that the right hemisphere underlies the temporal aspects of movement (Haaland et al. 1999) and contributes to the unilateral finger (Kim et al. 1993; Rao et al. 1993; Urbano et al. 1996; Cramer et al. 1999; Rogers et al. 2004; Hanakawa et al. 2005) and arm actions (Nirkko et al. 2001; Winstein et al. 1997).

Furthermore, larger SLF II in the right hemisphere corresponded to shorter deceleration duration and lower amplitude of closing grip velocity of reach-to-grasp movements. Consistent with the previous literature (Jakobson and Goodale 1991; Chieffi and Gentilucci 1993), faster deceleration was associated with faster closing grip velocity. Having in mind that the function of the limb deceleration is to achieve a stable final position for grasping the object (Brown and Cooke 1986; Cook and Brown 1990; Berardelli et al. 1996), our results suggest faster reach-grasp coordination in individuals with larger SLF II in the right hemisphere. This is also in line with the evidence that the cortical regions connected by this tract, that is, the right middle frontal gyrus and the right intraparietal regions are active during precision grasping (Begliomini et al. 2014). Furthermore, our findings support the role of the right hemisphere in grasp-preshaping (Tretriluxana et al. 2008; Begliomini et al. 2008), control of finger configurations (Goldenberg et al. 2001; Hermsdörfer et al. 2001; Della Sala et al. 2006), and final limb positions (Haaland et al. 2004; Schaefer et al. 2007, 2009; Mani et al. 2013; Mutha et al. 2013). Hence, besides the temporal aspects, the right SLF II might be important for the final arm position and the fingers closing phase around the target object. Previously, the right SLF II was implicated in visuospatial processing (Thiebaut de Schotten et al. 2005; Bartolomeo et al. 2007, 2012; Doricchi et al. 2008; Lunven et al. 2015), and the right inferior parietal cortex in working memory maintenance of grasp-related visuospatial information (Fiehler et al. 2011). Thus, the right SLF II could act as a substrate for coupling visuospatial information to the preparation of reach and grasp movements by integrating visuomotor and attention-related processes (Castiello 1998; Tipper et al. 1998).

Relating Variation in Kinematics with SLF II Hemispheric Distribution

Our study confirmed previously reported symmetrical distribution of the SLF II (Thiebaut de Schotten et al. 2011). High inter-individual variability allowed us to observe significant relationship between SLF II lateralization and the acceleration amplitudes of reach and reach-to-grasp movements. Larger SLF II in the right hemisphere relative to the left corresponded to higher movement acceleration amplitude—consistent with our findings on individual segments. This is the first demonstration that the asymmetry of the SLF II is implicated in the variability of initial movement trajectory during visuomotor processing. Previously, SLF II lateralization was found to predict the behavioral performance on visuospatial attention tasks (Thiebaut de Schotten et al. 2011). The lateralization of the SLF I and SLF III was not related to the movement kinematics. Right lateralization of the SLF III was consistent with the literature (Tomassini et al. 2007; Thiebaut de Schotten et al. 2011) but the left lateralization of the SLF I was in contrast to previous report of bilateral distribution (Thiebaut de Schotten et al. 2011). The reason for this discrepancy may lie

in high inter-individual variability associated with the SLF I measures in our study sample.

Further Implications

There are several other implications of our study. First, the fact that larger volumes of the right SLF II and SLF III were associated with faster speed of visuomotor processing could suggest several anatomical explanations. Larger tracts might have greater fiber myelination, higher number of axons, and larger axonal diameter that lead to higher conduction velocity (Waxman and Bennett 1972) and thus faster performance on reaching and reach-to-grasp tasks. This is in line with the previous tractography studies that found larger tracts associated with more effective connectivity and information transfer (Catani et al. 2007; Thiebaut de Schotten et al. 2011; López-Barroso et al. 2013). Secondly, our study has important implications on the functional correlates of the SLF in the human brain. The potential roles of SLF pathways are currently debated mostly based upon their cortical terminations and more rarely on clinico-anatomical correlations. Up till now, neuroimaging evidence showed that fronto-parietal pathways are important for tonic alertness and spatial attention (Sturm and Willmes 2001; Thiebaut de Schotten et al. 2011), visuospatial working memory (Darki and Klinberg 2014), explicit visuomotor learning (Bonzano et al. 2011), and tool use (Ramayya et al. 2010). Our study implicates the SLF pathways as important for the visuomotor processing during reach and reach-to-grasp movements. Lastly, our study aids in the shift of the prevalent cortical localization approach to the study of visuomotor processing of hand movements, toward a network model exploring the interconnectivity of cortical regions.

A Note on Limitations of the Study

There are technical limitations that need to be considered when interpreting the findings of the present study. First, the volumetric measures can depend on the underlying tractography algorithm and the experimental conditions (Jones and Cercignani 2010; Jones et al. 2012). Hence, it should be kept in mind that volume (i.e., the number of voxels intersected by streamline) does not represent the true tract volume but rather the spatial extent of the reconstructed tract, and likewise the number of streamlines is not a representation of true axonal fiber count. Also, since inter-subject variability can be substantial for diffusion measures, we recruited only right-handed subjects within a relatively narrow age range to further reduce the source of variability. Several anatomical factors such as crossing, kissing, or fanning fibers affect the ability to reconstruct the tracts and may lead to erroneous volumetric estimates. For this reason, we have used spherical deconvolution tractography that compared with the tensor approach models the diffusion signal as a distribution of multiple fiber orientations and is therefore able to resolve fiber crossing in regions with 2 or more tracts (Dell'Acqua et al. 2010). The use of this technique is especially well grounded when we have in mind that the number of voxels containing 2 or more fiber populations in the brain is estimated to be in the region of 90% (Jones et al. 2012). Nevertheless, tractography reconstructions based on the spherical deconvolution are still likely to generate false positives (Catani and Thiebaut de Schotten 2012). For that reason, all the tracts were visually inspected to confirm their known anatomical trajectories. It is still possible that smaller branches of the SLF were not reconstructed in our dataset, due to the limited spatial resolution and relatively large voxels, however repeating and averaging the measurements 3 times increased the signal-to-noise ratio. Further studies are needed to replicate our results on a larger data cohort, with the inclusion of functional neuroimaging measures.

Conclusion

Overall, the present study is the first to demonstrate that asymmetry and structure of the fronto-parietal white matter networks, namely the bilateral SLF II and SLF III, support upper limb movements such as reaching and reaching-to-grasp. The SLF II and SLF III in the right hemisphere were related to the temporal aspects of movement, while the left SLF II and SLF III played a role in initial trajectory features such as movement acceleration. Furthermore, the right SLF II was involved in the reach-grasp coordination and the closing grip phase of the movement, necessary for efficient and stable contact with the target object. Our study suggested that a key position between sensory and motor systems might allow SLF II and SLF III to act as a common network to support visuomotor processing required to generate both reach and reach-to-grasp movements.

Supplementary material

Supplementary material can be found at http://www.cercor.oxfordjournals.org/online.

Funding

This work was supported by a grant from the MIUR (N. 287713), the FP7: REWIRE project, and the Progetto Strategico, Università di Padova (N. 2010XPMFW4) to U.C.

Notes

We thank our laboratory coordinator Elisa Straulino for her help in recruiting the participants, and Luisa Sartori for helping us to perform the kinematic experiments. *Conflict of Interest*: None declared.

References

Alexander DC. 2005. Multiple-fiber reconstruction algorithms for diffusion MRI. Ann N Y Acad Sci. 1064:113–133.

Andersen RA, Buneo CA. 2002. Intentional maps in posterior parietal cortex. Annu Rev Neurosci. 25:189–220.

Bagesteiro LB, Sainburg RL. 2002. Handedness: dominant arm advantages in control of limb dynamics. J Neurophysiol. 88:2408–2421.

Bagesteiro LB, Sainburg RL. 2003. Nondominant arm advantages in load compensation during rapid elbow joint movements. J Neurophysiol. 90(3):1503–1513.

Bartolomeo P, Thiebaut de Schotten M, Chica AB. 2012. Brain networks of visuospatial attention and their disruption in visual neglect. Front Hum Neurosci. 6:110.

Bartolomeo P, Thiebaut de Schotten M, Doricchi F. 2007. Left unilateral neglect as a disconnection syndrome. Cereb Cortex. 17(11):2479–2490.

Begliomini C, Caria A, Grodd W, Castiello U. 2007. Comparing natural and constrained movements: new insights into the visuomotor control of grasping. PLoS One. 2(10):e1108.

Begliomini C, De Sanctis T, Marangon M, Tarantino V, Sartori L, Miotto D, Motta R, Stramare R, Castiello U. 2014. An investigation of the neural circuits underlying reaching and reach-to-

grasp movements: from planning to execution. Front Hum Neurosci. 8:676.
Begliomini C, Nelini C, Caria A, Grodd W, Castiello U. 2008. Cortical activations in humans grasp-related areas depend on hand used and handedness. PLoS One. 3(10):e3388.
Benjamini Y, Hochberg Y. 1995. Controlling the false discovery rate: a practical and powerful approach to multiple testing. J R Stat Soc Ser B (Methodological). 57(1):289–300.
Berardelli A, Hallett M, Rothwell JC, Agostino R, Manfredi M, Thompson PD, Marsden CD. 1996. Single-joint rapid arm movements in normal subjects and in patients with motor disorders. Brain. 119(Pt 2):661–674.
Binkofski F, Dohle C, Posse S, Stephan KM, Hefter H, Seitz RJ, Freund HJ. 1998. Human anterior intraparietal area subserves prehension: a combined lesion and functional MRI activation study. Neurology. 50(5):1253–1259.
Bonzano L, Tacchino A, Roccatagliata L, Sormani MP, Mancardi GL, Bove M. 2011. Impairment in explicit visuomotor sequence learning is related to loss of micro structural integrity of the corpus callosum in multiple sclerosis patients with minimal disability. Neuroimage. 57(2):495–501.
Borra E, Belmalih A, Calzavara R, Gerbella M, Murata A, Rozzi S, Luppino G. 2008. Cortical connections of the macaque anterior intraparietal (AIP) area. Cereb Cortex. 18(5):1094–1111.
Brown SH, Cooke JD. 1986. Initial agonist burst is modified by perturbations preceding movement. Brain Res. 377(2):311–322.
Buneo CA, Jarvis MR, Batista AP, Andersen RA. 2002. Direct visuomotor transformations for reaching. Nature. 416:632–636.
Buxbaum LJ, Kyle KM, Tang K, Detre JA. 2006. Neural substrates of knowledge of hand postures for object grasping and functional object use: evidence from fMRI. Brain Res. 1117(1):175–185.
Castiello U. 1998. Attentional coding for three-dimensional objects and two-dimensional shapes. Differential interference effects. Exp Brain Res. 123(3):289–297.
Castiello U. 2001. The effects of abrupt onset of 2-D and 3-D distractors on prehension movements. Percept Psychophys. 63(6):1014–1025.
Castiello U. 2005. The neuroscience of grasping. Nat Rev Neurosci. 6(9):726–736.
Castiello U, Begliomini C. 2008. The cortical control of visually guided grasping. Neuroscientist. 14(2):157–170.
Catani M, Allin MP, Husain M, Pugliese L, Mesulam MM, Murray RM, Jones DK. 2007. Symmetries in human brain language pathways correlate with verbal recall. Proc Natl Acad Sci USA. 104(43):17163–17168.
Catani M, Thiebaut de Schotten M. 2012. Atlas of human brain connections. Oxford: Oxford University Press.
Cavina-Pratesi C, Monaco S, Fattori P, Galletti C, McAdam TD, Quinlan DJ, Goodale MA, Culham JC. 2010. Functional magnetic resonance imaging reveals the neural substrates of arm transport and grip formation in reach-to-grasp actions in humans. J Neurosci. 30(31):10306–10323.
Chieffi S, Gentilucci M. 1993. Coordination between the transport and the grasp components during prehension movements. Exp Brain Res. 94(3):471–477.
Connolly JD, Andersen RA, Goodale MA. 2003. FMRI evidence for a "parietal reach region" in the human brain. Exp Brain Res. 153:140–145.
Cook JD, Brown SH. 1986. Phase plane tracking: a new method for shaping movements. Brain Res Bull. 16(3):435–437.
Cramer SC, Finklestein SP, Schaechter JD, Bush G, Rosen BR. 1999. Activation of distinct motor cortex regions during ipsilateral and contralateral finger movements. J Neurophysiol. 81 (1):383–387.
Culham JC, Valyear KF. 2006. Human parietal cortex in action. Curr Opin Neurobiol. 16(2):205–212.
Curtis CE, D'Esposito M. 2003. Persistent activity in the prefrontal cortex during working memory. Trends Cogn Sci. 7(9):415–423.
D'Amico M, Ferrigno G. 1992. Comparison between the more recent techniques for smoothing and derivative assessment in biomechanics. Med Biol Eng Comput. 30(2):193–204.
D'Amico M, Ferrigno G. 1990. Technique for evaluation of derivates from noisy biomechanical displacement data using model-based bandwith-selection procedure. Med Biol Eng Comput. 28(5):407–415.
Darki F, Klinberg T. 2014. The role of fronto-parietal and fronto-striatal networks in the development of working memory: a longitudinal study. Cereb Cortex. 25(6):1587–1595.
Davare M, Andres M, Cosnard G, Thonnard JL, Olivier E. 2006. Dissociating the role of ventral and dorsal premotor cortex in precision grasping. J Neurosci. 26(8):2260–2268.
Davare M, Duque J, Vandermeeren Y, Thonnard JL, Olivier E. 2007. Role of the ipsilateral primary motor cortex in controlling the timing of hand muscle recruitment. Cereb Cortex. 17 (2):353–362.
Davare M, Kraskov A, Rothwell JC, Lemon RN. 2011. Interactions between areas of the cortical grasping network. Curr Opin Neurobiol. 21(4):565–570.
Dell'Acqua F, Scifo P, Rizzo G, Catani M, Simmons A, Scotti G, Fazio F. 2010. A modified damped Richardson-Lucy algorithm to reduce isotropic background effects in spherical deconvolution. Neuroimage. 49(2):1446–1458.
Dell'Acqua F, Simmons A, Williams SC, Catani M. 2013. Can spherical deconvolution provide more information that fiber orientations? Hindrance modulated orientational anisotropy, a true-tract specific index to characterize white matter diffusion. Hum Brain Mapp. 34(10):2464–2483.
Della Sala S, Faglioni P, Motto C, Spinnler H. 2006. Hemisphere asymmetry for imitation of hand and finger movements, Goldenberg's hypothesis reworked. Neuropsychologia. 44 (8):1496–1500.
Doricchi F, Thiebaut de Schotten M, Tomaiuolo F, Bartolomeo P. 2008. White matter (dis)connections and gray matter (dys) functions in visual neglect: gaining insights into the brain networks of spatial awareness. Cortex. 44(8):983–995.
Ehrsson HH, Fagergren E, Forssberg H. 2001. Differential fronto-parietal activation depending on force used in a precision grip task: an fMRI study. J Neurophysiol. 85(6):2613–2623.
Ehrsson HH, Fagergren A, Jonsson T, Westling G, Johansson RS, Forssberg H. 2000. Cortical activity in precision- versus power-grip tasks: an fMRI study. J Neurophysiol. 83(1):528–536.
Fabbri S, Strnad L, Caramazza A, Lingnau A. 2014. Overlapping representations for grip type and reach direction. Neuroimage. 94:138–146.
Fattori P, Breveglieri R, Amoroso K, Galletti C. 2004. Evidence for both reaching and grasping activity in the medial parieto-occipital cortex of the macaque. Eur J Neurosci. 20(9):2457–2466.
Fattori P, Breveglieri R, Marzocchi N, Filippini D, Bosco A, Galletti C. 2009. Hand orientation during reach-to-grasp movements modulates neuronal activity in the medial posterior parietal area V6A. J Neurosci. 29(6):1928–1936.
Fattori P, Breveglieri R, Raos V, Bosco A, Galletti C. 2012. Vision for action in the macaque medial posterior parietal cortex. J Neurosci. 32(9):3221–3234.
Fattori P, Raos V, Breveglieri R, Bosco A, Marzocchi N, Galletti C. 2010. The dorsomedial pathway is not just for reaching: grasping neurons in the medial parieto-occipital cortex of the macaque monkey. J Neurosci. 30(1):342–349.

Fiehler K, Bannert MM, Bischoff M, Blecker C, Stark R, Vaitl D, Franz VH, Rosler F. 2011. Working memory maintenance of grasp-target information in the human posterior parietal cortex. Neuroimage. 54:2401–2411.

Filimon F. 2010. Human cortical control of hand movements: parietofrontal networks for reaching, grasping, and pointing. Neuroscientist. 16(4):388–407.

Fisk JD, Goodale MA. 1988. The effects of unilateral brain damage on visually guided reaching: hemispheric differences in the nature of the deficit. Exp Brain Res. 72:425–435.

Gamberini M, Passarelli L, Fattori P, Zucchelli M, Bakola S, Luppino G, Galletti C. 2009. Cortical connections of the visuomotor parietooccipital area V6Ad od the macaque monkey. J Comp Neurol. 513(6):622–642.

Gentilucci M, Castiello U, Corradini ML, Scarpa M, Umiltà C, Rizzolatti G. 1991. Influence of different types of grasping on the transport component of prehension movements. Neuropsychologia. 29(5):361–378.

Glover S, Wall MB, Smith AT. 2012. Distinct cortical networks support the planning and online control of reaching-to-grasp in humans. Eur J Neurosci. 35(6):909–915.

Goldenberg G, Laimgruber K, Hermsdörfer J. 2001. Imitation of gestures by disconnected hemispheres. Neuropsychologia. 39(13):1432–1443.

Grafton ST. 2010. The cognitive neuroscience of prehension: recent developments. Exp Brain Res. 204(4):475–491.

Grol MJ, Majdandzic J, Stephan KE, Verhagen L, Dijkerman HC, Bekkering H, Verstraten FA, Toni I. 2007. Parieto-frontal connectivity during visually guided grasping. J Neurosci. 27 (44):11877–11887.

Haaland KY, Harrington DL. 1989. Hemispheric control of the initial and corrective components of aiming movements. Neuropsychologia. 27(7):961–969.

Haaland KY, Harrington DL, Knight RT. 1999. Spatial deficits in ideomotor limb apraxia. A kinematic analysis of aiming movements. Brain. 122:1169–1182.

Haaland KY, Prestopnik JL, Knight RT, Lee RR. 2004. Hemispheric asymmetries for kinematic and positional aspects of reaching. Brain. 127:1145–1158.

Hanakawa T, Parikh S, Bruno MK, Hallett M. 2005. Finger and face representations in the ipsilateral pre central motor areas in humans. J Neurophysiol. 93(5):2950–2958.

Hermsdörfer J, Goldenberg G, Wachsmuth C, Conrad B, Ceballos-Baumann AO, Bartenstein P, Schwaiger M, Boecker H. 2001. Cortical correlates of gesture processing: clues to the cerebral mechanisms underlying apraxia during imitation of meaningless gestures. Neuroimage. 14(Pt 1):149–161.

Jakobson LS, Goodale MA. 1991. Factors affecting higher-order movement planning: a kinematic analysis of human prehension. Exp Brain Res. 86(1):199–208.

Jang SH, Hong JH. 2012. The anatomical characteristics of superior longitudinal fasciculus I in human brain: diffusion tensor tractography study. Neurosci Lett. 506(1):146–148.

Jeannerod M, Arbib MA, Rizzolatti G, Sakata H. 1995. Grasping objects: the cortical mechanisms of visuomotor transformation. Trends Neurosci. 18(7):314–320.

Jones DK, Cercignani M. 2010. Twenty-five pitfalls in the analysis of diffusion MRI data. NMR Biomed. 23(7):803–820.

Jones DK, Knösche TR, Turner R. 2012. White matter integrity, fiber count, and other fallacies: the do's and don'ts of diffusion MRI. Neuroimage. 73:239–254.

Kakei S, Hoffman DS, Strick PL. 2001. Direction of action is represented in the ventral premotor cortex. Nat Neurosci. 4 (10):1020–1025.

Kamali A, Flanders AE, Brody J, Hunter JV, Hasan KM. 2014. Tracing superior longitudinal fasciculus connectivity in the human brain using high resolution diffusion tensor tractography. Brain Struct Funct. 219(1):269–281.

Karnath HO, Perenin MT. 2005. Cortical control of visually guided reaching: evidence from patients with optic ataxia. Cereb Cortex. 15(10):1561–1569.

Kim SG, Ashe J, Georgopoulos AP, Merkle H, Ellermann JM, Menon RS, Ogawa S, Ugurbil K. 1993. Functional imaging of human motor cortex at high magnetic field. J Neurophysiol. 69(1):297–302.

Koch G, Cercignani M, Pecchioli C, Versace V, Oliveri M, Caltagirone C, Rothwell J, Bozzali M. 2010. In vivo definition of parieto-motor connections involved in planning of grasping movements. Neuroimage. 51(1):300–312.

Konczak J, Karnath HO. 1998. Kinematics of goal-directed arm movements in neglect: control of hand velocity. Brain Cogn. 37(3):387–403.

Lau HC, Rogers RD, Ramnani N, Passingham RE. 2004. Willed action and attention to the selection of action. Neuroimage. 21 (4):1407–1415.

Lee IA, Preacher KJ. 2013. Calculation for the test of the difference between two dependent correlations with one variable in common [Computer software]. http://quantpsy.org, last accessed May, 2015.

Leemans A, Jeurissen B, Sijbers J, Jones DK. 2009. ExploreDTI: a graphical toolbox for processing, analyzing, and visualizing diffusion MR data. In: 17th Annual Meeting of Intl Soc Mag Reson Med. Hawaii, USA. 3537 p.

López-Barroso D, Catani M, Ripollés P, Dell'Acqua F, Rodríguez-Fornells A, de Diego-Balaguer R. 2013. Word learning is mediated by the left arcuate fasciculus. Proc Natl Acad Sci USA. 110(32):13168–13173.

Lunven M, Thiebaut De Schotten M, Bourlon C, Duret C, Migliaccio R, Rode G, Bartolomeo P. 2015. White matter lesional predictors of chronic visual neglect: a longitudinal study. Brain. 138(Pt 3):746–760.

Makris N, Kennedy DN, McInerney S, Sorensen AG, Wang R, Caviness VS Jr, Pandya DN. 2005. Segmentation of subcomponents within the superior longitudinal fascicle in humans: a quantitative, in vivo, DT-MRI study. Cereb Cortex. 15(6):854–869.

Mani S, Mutha PK, Przybyla A, Haaland KY, Good DC, Sainburg RL. 2013. Contralesional motor deficits after unilateral stroke reflect hemisphere-specific control mechanisms. Brain. 136(Pt 4):1288–1303.

Marteniuk RG, MacKenzie CL, Jeannerod M, Athenes S, Dugas C. 1987. Constraints on human arm movement trajectories. Can J Psychol. 41(3):365–378.

Martin K, Jacobs S, Frey HS. 2011. Handedness-dependent and -independent cerebral asymmetries in the anterior intraparietal sulcus and ventral premotor cortex during grasp planning. Neuroimage. 57(2):502–512.

Matelli M, Govoni P, Galletti C, Kutz DF, Luppino G. 1998. Superior area 6 afferents from the superior parietal lobule in the macaque monkey. J Comp Neurol. 402(3):327–352.

Matelli M, Luppino G. 2001. Parietofrontal circuits for action and space perception in the macaque monkey. Neuroimage. 14(1 Pt 2):S27–S32.

Mattingley JB, Phillips JG, Bradshaw JL. 1994. Impairments of movement execution in unilateral neglect: A kinematic analysis of directional bradykinesia. Neuropsychologia. 32(9):1111–1134.

Monaco S, Chen Y, Medendorp WP, Crawford JD, Fiehler K, Henriques DY. 2014. Functional magnetic resonance imaging

adaptation reveals the cortical networks for processing grasp-relevant object properties. Cereb Cortex. 24(6):1540–1554.
Mutha PK, Haaland KY, Sainburg RL. 2013. Rethinking motor lateralization: specialized but complementary mechanisms for motor control of each arm. PLoS One. 8(3):e58582.
Nirkko AC, Ozdoba C, Redmond SM, Burki M, Schroth G, Hess CW, Wiesendanger M. 2001. Differential ipsilateral representations for distal and proximal movements in the sensorimotor cortex: activation and deactivation patterns. Neuroimage. 13:825–835.
Oldfield RC. 1971. The assessment and analysis of handedness: the Edinburgh inventory. Neuropsychologia. 9(1):97–113.
Olivier E, Davare M, Andres M, Fadiga L. 2007. Precision grasping in humans: from motor control to cognition. Curr Opin Neurobiol. 17(6):644–648.
Passarelli L, Rosa MG, Gamberini M, Bakola S, Burman KJ, Fattori P, Galletti C. 2011. Cortical connections of area V6Av in the macaque: a visual-input node to the eye/hand coordination system. J Neurosci. 31(5):1790–1801.
Petrides M, Pandya DN. 1984. Projections to the frontal cortex from the posterior parietal region in the rhesus monkey. J Comp Neurol. 228(1):105–116.
Ramayya AG, Glasser MF, Rilling JK. 2010. A DTI investigation of neural substrates supporting tool use. Cereb Cortex. 20 (3):507–516.
Rao SM, Binder JR, Bandettini PA, Hammeke TA, Yetkin FZ, Jesmanowicz A, Lisk LM, Morris GL, Mueller WM, Estkowski LD, et al. 1993. Functional magnetic resonance imaging of complex human movements. Neurology. 43(11):2311–2318.
Raos V, Umiltá MA, Murata A, Fogassi L, Gallese V. 2006. Functional properties of grasping-related neurons in the ventral premotor area F5 of the macaque monkey. J Neurophysiol. 95(2):709–729.
Rizzolatti G, Luppino G. 2001. The cortical motor system. Neuron. 31(6):889–901.
Robertson JV, Rohe N, Roby-Brami A. 2012. Influence of the side of brain damage on postural upper-limb control including the scapula in stroke patients. Exp Brain Res. 218:141–155.
Rogers BP, Carew JD, Meyerand ME. 2004. Hemispheric asymmetry in supplementary motor area connectivity during unilateral finger movements. Neuroimage. 22(2):855–859.
Rojkova K, Volle E, Urbanski M, Humbert F, Dell'Acqua F, Thiebaut de Schotten M. 2015. Atlasing the frontal lobe connections and their variability due to age and education: a spherical deconvolution tractography study. Brain Struct Funct. doi:10.1007/s00429-015-1001-3.
Rushworth MF, Nixon PD, Renowden S, Wade DT, Passingham RE. 1997. The left parietal cortex and motor attention. Neuropsychologia. 35(9):1261–1273.
Rushworth MFS, Krams M, Passingham RE. 2001. The attentional role of the left parietal cortex: the distinct lateralization and localization of motor attention in the human brain. J Cogn Neurosci. 13(5):698–710.
Sainburg RL. 2002. Evidence for a dynamic-dominance hypothesis of handedness. Exp Brain Res. 142:241–258.
Sainburg RL, Kalakanis D. 2000. Differences in control of limb dybamics during dominant and nondominant arm reaching. J Neurophysiol. 83:2661–2675.
Sainburg RL, Wang J. 2002. Interlimb transfer of visuomotor rotations: independence of direction and final position information. Exp Brain Res. 145:437–447.
Schaefer SY, Haaland KY, Sainburg RL. 2009. Dissociation of initial trajectory and final position errors during visuomotor adaptation following unilateral stroke. Brain Res. 1321: 180–181.
Schaefer SY, Haaland KY, Sainburg RL. 2007. Ipsilesional motor deficits following stroke reflect hemispheric specializations for movement control. Brain. 130(Pt 8):2146–2158.
Shapiro SS, Wilk MB. 1965. Analysis of variance test for normality (complete samples). Biometrika. 52(3/4):591–611.
Sturm W, Willmes K. 2001. On the functional neuroanatomy of intrinsic and phasic alertness. Neuroimage. 14(1 Pt 2):S76–S84.
Tarantino V, De Sanctis T, Straulino E, Begliomini C, Castiello U. 2014. Object size modulate sfronto-parietal activity during reaching movements. Eur J Neurosci. 39(9):1528–1537.
Thiebaut de Schotten M, Dell'Acqua F, Forkel SJ, Simmons A, Vergani F, Murphy DG, Catani M. 2011. A lateralized brain network for visuospatial attention. Nat Neurosci. 14 (10):1245–1246.
Thiebaut de Schotten M, Dell'Acqua F, Valabregue R, Catani M. 2012. Monkey to human comparative anatomy of the frontal lobe association tracts. Cortex. 48(1):82–96.
Thiebaut de Schotten M, Urbanski M, Duffau H, Volle E, Lévy R, Dubois B, Bartolomeo P. 2005. Direct evidence for a parietal-frontal pathway subserving spatial awareness in humans. Science. 309(5744):2226–2228.
Tipper SP, Howard LA, Houghton G. 1998. Action-based mechanisms of attention. Philos Trans R Soc Lond B Biol Sci. 353 (1373):1358–1393.
Tomassini V, Jbabdi S, Klein JC, Behrens TE, Pozzilli C, Matthews PM, Rushworth MF, Johansen-Berg H. 2007. Diffusion-weighted imaging tractography-based parcellation of the human lateral premotor cortex identifies dorsal and ventral subregions with anatomical and functional specializations. J Neurosci. 27(38):10259–10269.
Tournier JD, Calamante F, Connelly A. 2007. Robust determination of the fibre orientation distribution in diffusion MRI: non-negativity constrained super-resolved spherical deconvolution. Neuroimage. 35(4):1459–1472.
Tournier JD, Calamante F, Gadian DG, Connelly A. 2004. Direct estimation of the fiber orientation density function from diffusion-weighted MRI data using spherical deconvolution. Neuroimage. 23(3):1176–1185.
Tretriluxana J, Gordon J, Winstein CJ. 2008. Manual asymmetries in grasp-shaping and transport-grasp coordination. Exp Brain Res. 188(2):205–315.
Urbano A, Babiloni C, Onorati P, Babiloni F. 1996. Human cortical activity related to unilateral movements. A high resolution EEG Study. Neuroreport. 8(1):203–206.
Wang R, Benner T, Sorensen AG, Wedeen VJ. 2007. Diffusion Toolkit: a software package for diffusion imaging data processing and tractography. Proc Intl Soc Mag Reson Med. 15:3720.
Wang X, Pathak S, Stefaneanu L, Yeh FC, Li S, Fernandez-Miranda JC. 2015. Subcomponents and connectivity of the superior longitudinal fasciculus in the human brain. Brain Struct Funct. PMID:25782434. [Epub ahead of print].
Winstein CJ, Grafton ST, Pohl PS. 1997. Motor task difficulty and brain activity: investigation of goal-directed reciprocal aiming using positron emission tomography. J Neurophysiol. 77:1581–1594.
Waxman SG, Bennett MV. 1972. Relative conduction velocities of small myelinated and non-myelinated fibres in the central nervous system. Nat New Biol. 238(85):217–219.
Winstein CJ, Pohl PS. 1995. Effects of unilateral brain damage on the control of goal-directed hand movements. Exp Brain Res. 105(1):163–174.